



Numerical Study of Hypersonic Laminar Interaction Induced by the Swept Blunt Fins

Y. L. Liu^(✉) and J. K. Ma

China Academy of Aerospace Aerodynamics, Beijing, China
lyf545@sohu.com

Abstract. The laminar interaction hypersonic flowfield induced by the sweep blunt fins, which are mounted on the flat plate, is numerical studied. Finite volume method and multi-block patched meshes are used to solve three dimensional compressible Navier-Stokes equations. The influence of grid density, numerical schemes and limiter functions are studied. Spatial structure and surface flow separation pattern are described and the influence of different sweep angles is also given. The results show that grid numbers, numerical schemes and limiter functions have huge impact on the computation results. On the basis of the computational stability, high density grid numbers, low dissipation numerical schemes and limiter functions are preferred to obtain a proper result. For the interaction flowfield, the extent of the separation region and the peak value of the heat flux are decreased as the sweep angles increase.

Keywords: Hypersonic flow · The swept blunt fins · Shock wave/boundary layer interaction

1 Introduction

Aero-rudders are often used in hypersonic vehicles usually use to change flight trajectories and flight attitude. When the super-hypersonic flow passes through the aero-rudders, there are complex flow phenomena such as shock wave/boundary layer interaction, shock/shock interaction, flow separation and reattachment in the flow field [1]. The pressure and heat flow load in the disturbed area are obviously changed, and the unsteady flow characteristics are obviously [2, 3]. These characteristics make it difficult to determine the aerodynamic characteristics and structural design of the aircraft.

In order to facilitate the research, aircraft wing/body interference is usually simplified as a sharp fin or blunt fin mounted on the plate. In the past few decades, the study of the interaction flow field of the blunt fin has been paid much attention. A great deal of theoretical analysis, calculation and experiment have been carried out at home and abroad, but most of the research focuses on the turbulent flow field, and the results of the laminar flow interference are few. In recent years, near space hypersonic vehicles, such as HTV-2 in the United States, have been developed vigorously in the United States. The flow field of the aircraft is in a laminar state for quite a long time as the flow Reynolds number is low in the near space. Therefore, it is important to understand the characteristics of the laminar flow field for the design of such aircraft.

In view of the interaction characteristics of hypersonic blunt fin laminar flow, researchers at home and abroad have studied. Li Suxun and other [4, 5] measured the pressure distribution and surface heat flow rate distribution of the laminar interaction flow field of $Ma = 8.0$ with the blunt fin through a wind tunnel experiment. The results show that the range of laminar interaction region is far greater than the turbulence interaction area. The pressure and heat load distribution is also different from that in the turbulence. Schuricht [6] also measured the surface heat flow rate of the blunt fin laminar interaction flow field under $Ma = 6.7$. The experimental results show that the structure of the laminar interaction flow is complex and the interference range reaches the diameter of the 7 times fin leading edge in the upstream of the blunt fin. The peak value of the heat transfer rate can reach 7 times of the thermal flow rate in the undisturbed area. The numerical effects of the laminar flow around the hypersonic biconical model have been studied systematically by Druguet and Candler [7]. It is found that different numerical methods have a great influence on the accurate prediction of flow separation. Under the same grid and numerical schemes, with the less dissipation of the limiter and the higher the calculation precision, the separation flow can be better captured. But the low dissipation is easy to cause the oscillation of the calculation result and difficult to converge.

In this paper, the laminar interference characteristics of a blunt fin mounted on a flat plate under hypersonic condition are numerically studied. Through the comparison with the experimental results, the influence of numerical factors (grid, numerical scheme and limiter) on the laminar flow interaction characteristics is obtained. The numerical simulation of Ausmpw+ scheme and Vanleer limiters is given. The influence of the disturbance range and the distribution of heat flow rate on the flow field of the swept angle is analyzed. The results can provide reference and basis for the engineering design.

2 Numerical Methods and Model

2.1 Numerical Methods

The three-dimensional compressible laminar Navier-Stokes equations in curvilinear coordinates are solved with finite volume discretization and multi-block grid technology. The viscosity terms are discretized by the central difference scheme, and the discretization of time derivative terms is realized by implicit LU-SGS method. The spatial discretization schemes used in the calculation include Roe scheme, Ausmpw+ scheme and Van leer scheme. The spatial scheme is improved to two order precision by MUSCL interpolation. The limiter functions used include: minmod limiter, van leer limiter, double minmod limiter. The detailed algorithm can be found in [8, 9].

2.2 Boundary Conditions

1. **Inlet boundary:** The static pressure, static temperature and the Mahler number of incoming flow are given at the inlet boundary.

2. **Out flow boundary:** When the outlet is hypersonic or hypersonic, the downstream flow field does not affect the upstream flow field, and interpolate all the parameter values.
3. **Solid wall boundary:** No slip condition is adopted, and temperature is treated as isothermal wall.
4. **Symmetric boundary:** The normal velocity is zero on the symmetric plane, and the normal gradient of all variables is zero.

2.3 Model and Conditions

A hypersonic test model is used in the paper. The model has completed the heat measurement, high speed schlieren and pressure measurement [10] in the FD-20 of the hypersonic gun wind tunnel of CAAA. The model and coordinate system are showed in Fig. 1. The model is composed of a flat plate and a swept angle $\Lambda = 45^\circ$ blunt fin model. the plate is 680 mm long and 380 mm wide. The leading edge of the fin is 432.5 mm at the front end of the plate and the diameter of the fin leading edge is $D = 25$ mm, and the swept angle of the fin is $\Lambda = 45^\circ$. According to the symmetry of the flow field, the calculated area is half of the model along the symmetry plane. The origin of coordinates is taken at the center line of the leading edge of the rudder leading to the intersection of the center line of the plate. The data on the flat plate uses the OXYZ coordinate system, in which the OX coordinates are directed down the center line of the flat plate, and the OY coordinates are perpendicular to the plate direction. The OZ is perpendicular to the OX and OY and forms the right hand coordinate system. The data on the rudder surface are in the OSYZ coordinate system, where the OS coordinates move along the center line of the front edge of the fin, pointing to the direction far away from the plate.

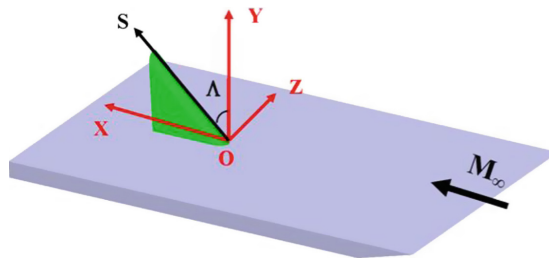


Fig. 1. Model and coordinate system

The calculation conditions are shown in Table 1. From the surface heat flow rate distribution of the plate model obtained under the same experimental conditions [11] it can be determined that the state of the local plate boundary layer at the intersection of the center line of the fin front and the center line of the flat plate is laminar flow.

Table 1. The calculation conditions

Ma	P ₀ (Mpa)	T ₀ (K)	T _{wall} (K)	Re/m
8.0	6.0	1093	290	7.1×10^6

3 Results and Analysis

3.1 Analysis of Numerical Influencing Factors

The interaction flow field of the shock wave/boundary layer caused by the finis is very complicated. There is a complex wave system with separation shock wave and bow shock wave. At the same time, the flow separation and reattachment are usually found in the disturbance flow field, and the vortex in the separation area exists. Compared with turbulent flow field, laminar separation is more likely to occur under laminar flow conditions, and laminar flow separation is much larger than turbulent separation. The hypersonic/shock/boundary layer interaction is complicated and difficult to simulate accurately, which poses a challenge for numerical methods. The existing research results show that [7], grid, numerical scheme and limiter selection are important factors affecting the accurate prediction of laminar flow separation flow field, and the separation range from different numerical methods is very different.

In order to analyze the influence of grid factors, four sets of grid Grid1–Grid4 with different density are generated. The basic topology of different grids is the same and Normal first layer grid space is the same (fixed as 0.001 mm), and the number of grids is different. Figure 2 shows the grid structure of the model surface and the symmetry plane. In Table 2, the number of grid points in the streamwise direction (N_x), the number of grid points along the leading edge of the fin (N_y) and the number of points in the spanwise direction (N_z) are listed. The number of grid points on the rear edge of the fin to the flat edge is fixed to 31. The number of grid points along the normal direction is fixed to 31 above the fin and the number of grid points.

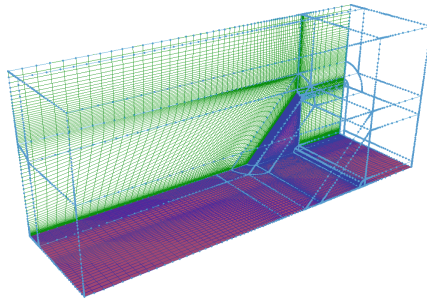
**Fig. 2.** Grid topology

Table 2. Grid number

	Nx	Ny	Nz
Grid1	81	61	61
Grid2	101	81	81
Grid3	121	101	101
Grid4	141	121	121

There are very complex flow phenomena such as leading shock wave, separation shock wave and flow separation in shock wave/boundary layer interaction flow. For numerical simulation, numerical dissipation is contained in numerical schemes and limiters to suppress the non physical oscillation produced by strong discontinuity such as shock waves and to improve the computational stability. However, the numerical dissipation can reduce the resolution of the flow characteristics such as shock and separation flow, and even conceal the real physical phenomena. The dissipation characteristics of numerical methods have great influence on the simulation accuracy of such problems.

By comparing the results of pressure distribution, separation distance and heat flux distribution obtained by different numerical schemes and limiter combinations, the influence of dissipation is analyzed with the experimental results. The numerical schemes include Ausmpw+ , Roe, Van leer, and the limiter function include double min mod limiter, van leer limiter and min mod limiter.

Figure 3 shows the pressure distribution along the center line of the plate under different grid densities and different numerical combinations. It can be seen from these results that the pressure distribution calculated under different grid density conditions, such as Roe scheme and min mod limiter, Van leer scheme and min mod limiter, are very different, and the difference of pressure distribution results gradually decreases with the increase of grid density. The results of pressure distribution calculated under different grid densities, such as the combination of Ausmpw+ scheme and van leer limiter, have little difference. Figure 4 shows the separation distance L calculated by different grids, numerical schemes and limiters. In this paper, the separation distance L is defined as the distance between the starting position of the load change of the model center line (compared with the plate model) to the fin root. The separation distance obtained in the experiment is L 50 mm. As we can see from Fig. 4, with the increase of grid density, the separation distance obtained by different numerical schemes and limiter combinations tends to experimental results. Under the same grid density conditions, the results obtained by the smaller dissipative scheme and the limiter combination are closer to the experimental values, and the change with the grid density is smaller.

Through the above analysis, we can see that in order to get more accurate results, we need to use densely grid, less dissipation numerical scheme and limiter combination. However, in the actual calculation, with the further increasing of the grid density on the basis of Grid4, the unstable phenomena such as non physical oscillation are found using low dissipation numerical scheme and limiter combination. Under the condition of this study, with the Grid4 grid density, the combination of the smaller dissipative numerical scheme and the limiter, such as the combination of the Ausmpw+ and the vanleer limiter, can obtain the better results of the pressure distribution and the separation distance. The subsequent calculation selects the Grid4 grid.

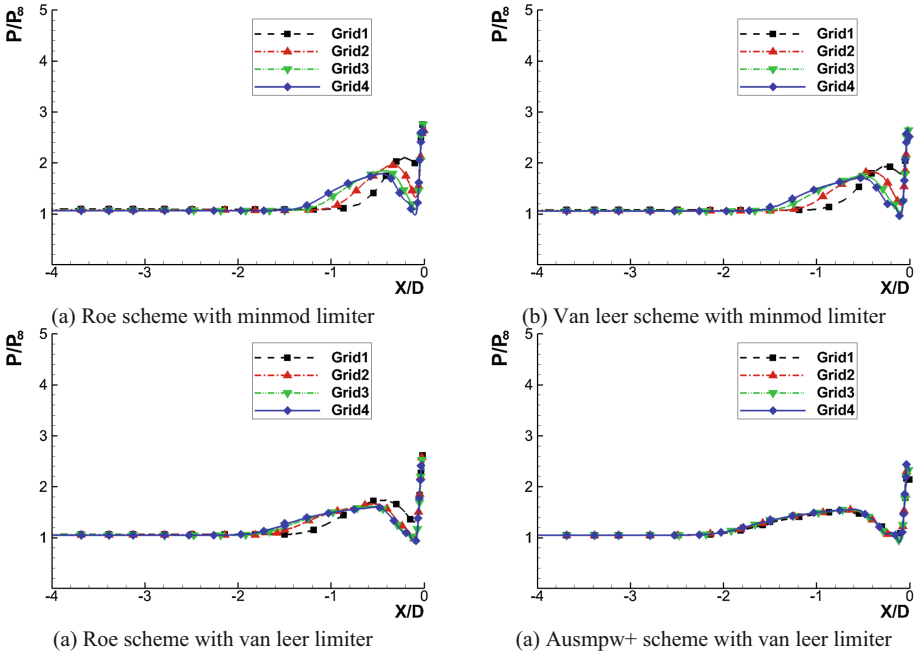


Fig. 3. Pressure distribution with different grids

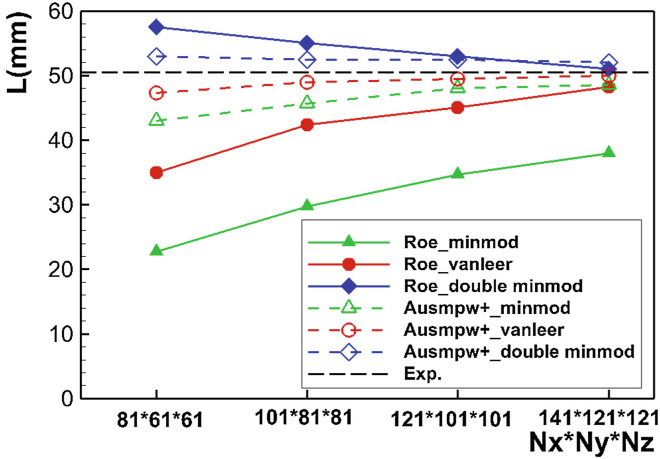


Fig. 4. Main separation distance

In Figs. 5 and 6, the heat transfer rate distribution on the surface of the center line and the center line of the leading edge of the fin is calculated and compared with the experimental data with the grid4 and minmod limiter. It can be seen that the Roe scheme and the Van leer scheme obviously overestimate the heat flow rate, and the Ausmpw+ scheme calculation is in good agreement with the test.

In Figs. 7 and 8, the heat transfer rate distribution on the surface of the center line and the center line of the leading edge of the fin is calculated and compared with the experimental data with the grid4 and van leer limiter. It can be seen that when the less dissipation van leer limiter is used, the results calculated by the three schemes are in good agreement with the experimental results. In comparison, the heat flux distribution on the center line of the plate and the center line of the leading edge of the fin calculated by the Ausmpw+ format is closer to the experimental results.

In Figs. 9 and 10, the heat transfer rate distribution on the surface of the center line and the center line of the leading edge of the fin is calculated and compared with the experimental data with the grid4 and double min mod limiter respectively. When the less dissipative double min mod limiter is used, the calculation is in good agreement with the experiment, but the combination of the Roe and the double minmod limiter is under-estimated the peak value in the position of the plate near the fin root, and there is a great oscillation in the heat transfer distribution curve of the fin upwind surface obtained by the combination of the Van leer scheme and the double minmod limiter. The results of the calculation deviate from the experimental results.

The calculation accuracy and stability are taken into consideration According to the calculation of the separation distance and the distribution of heat flux, and also

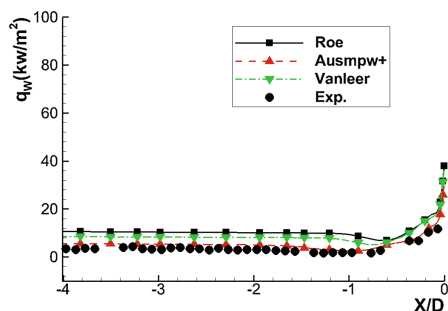


Fig. 5. Heat transfer rate distribution on the centerline of the plate (minmod limiter)

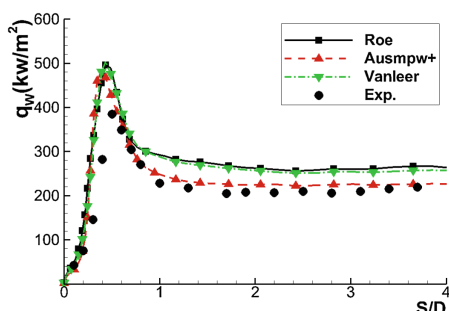


Fig. 6. Heat transfer rate distribution on the centerline of the fin (minmod limiter)

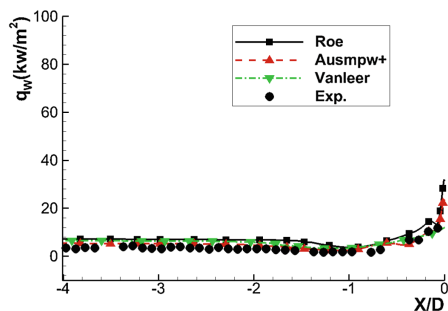


Fig. 7. Heat transfer rate distribution on the centerline of the plate (vanleer limiter)

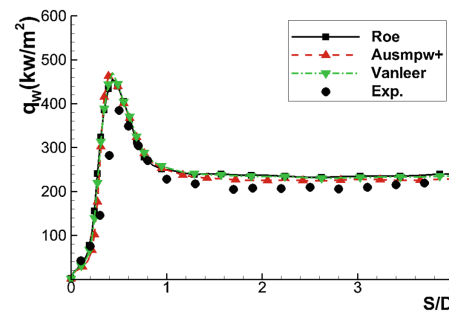


Fig. 8. Heat transfer rate distribution on the centerline of the fin (vanleer limiter)

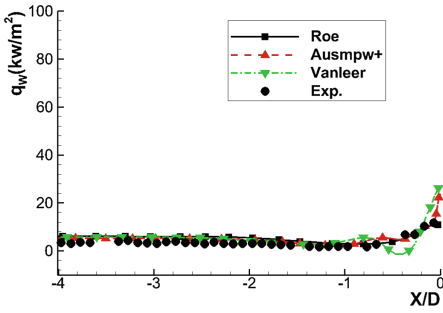


Fig. 9. Heat transfer rate distribution on the centerline of the plate (double minmod limiter)

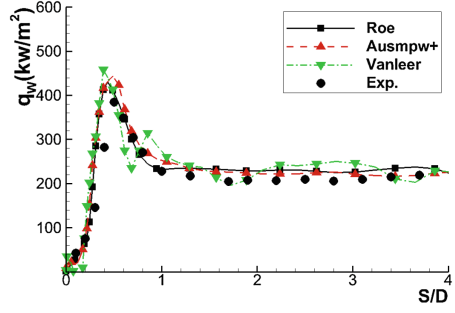


Fig. 10. Heat transfer rate distribution on the centerline of the fin (double minmod limiter)

calculation accuracy and stability are taken into consideration, the calculation results in the following are chosen by the combination of grid grid4, Ausmpw+ scheme and van leer limiter.

3.2 Surface and Spatial Interaction Flow Field Characteristics

Figure 11 shows the calculated shock wave/boundary layer interaction flow field caused by the blunt fin interaction using combination of the grid grid4, the Ausmpw+ scheme and the van leer limiter. Due to the interference of the blunt fin to the flow, A bow shock wave is formed ahead of the leading edge of the fin, and the inverse pressure gradient produced by the fin leading shock wave propagates upstream through the subsonic velocity zone in the boundary layer. The laminar boundary layer is weak in resistance to separation. The inverse pressure gradient often causes the separation of the boundary layer, and the separation shock wave is formed. The pressure rises after the separation of the separation wave, and there is a pressure peak near the position of the reattached line, as shown in Fig. 3. The separation shock intersects the shock in front of the fin leading to a complex “•” wave system, forming a tri-point structure. There is pressure and heat flux peak at the front of the fin leading edge. When the swept angle of blunt fin is small, the disturbance caused by blunt fin is strong, and the wave structure is obvious in the flow field.

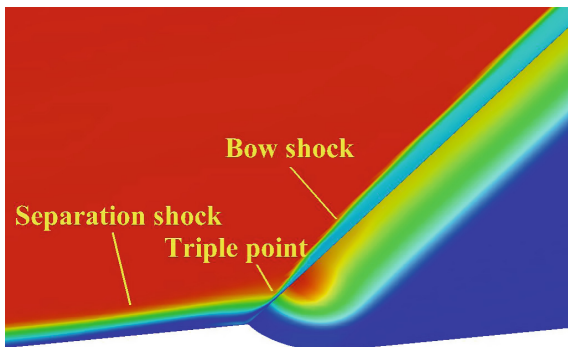


Fig. 11. Typical flow structure

Figures 12 and 13 give the schlieren photographs and the calculated density gradient contours of the $\Lambda = 45^\circ$ blunt fin under the same incoming flow condition. There is an obvious complex wave structure in the disturbance flow field of $\Lambda = 45^\circ$ blunt fin. Compared with the two photographs, the main flow structure, such as the fin leading edge shock wave the separation shock wave is in agreement with the experiment.

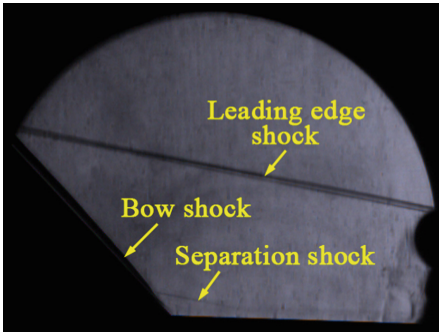


Fig. 12. Schlieren photograph

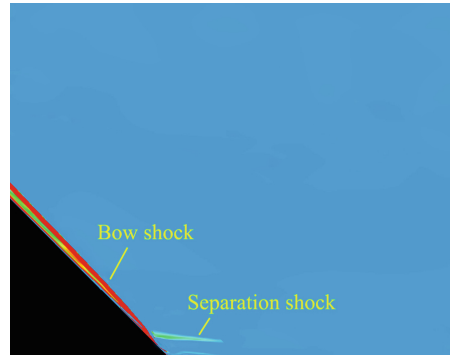


Fig. 13. Density gradient contours

Figure 14 shows the calculated limiting streamline diagram and the heat transfer rate contours on the plate of $\Lambda = 45^\circ$ model. It can be seen that there is a clear reverse flow area in front of the fin, and the main separation distance is about $1.6D$. The range of heat transfer rate interaction area is larger than that of the separation area. The distance of the initial interference point of the heat transfer rate in the center line of the plate is about $2.07D$, which is close to the results obtained by the experimental measurements ($2D$).

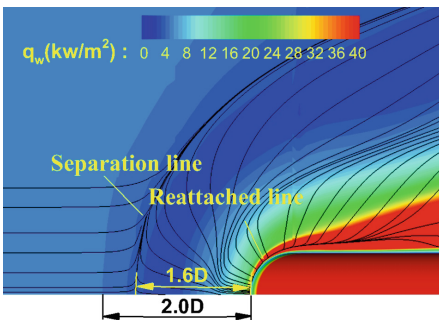


Fig. 14. Surface limiting streamline

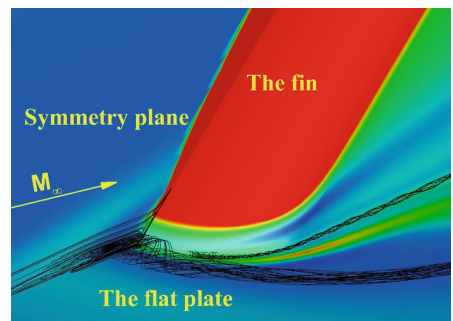


Fig. 15. Spatial streamline

Figure 15 gives the calculated spatial streamline and the pressure contours. This figure describes the typical spatial and wave systems of the disturbed flow field. Because of the interference of the blunt fin to the main stream, the boundary layer is separated at the upstream of the blunt fin. The horseshoe shaped separation vortex is tightly attached to the wall and bypasses the downstream development of the blunt fin. There is a small vortex between the blunt fin and the horseshoe separated vortex, which develops backward through the blunt fin. The spatial area of the blunt fin jamming increases with the vortex developing downstream.

3.3 Influence of the Sweep Angle

Figures 16 and 17 give the schlieren photos and calculated density gradient images of the $\Lambda = 67.5^\circ$ blunt fin under the same incoming flow condition. It can be seen that the intensity of the separation shock becomes weaker due to the weakening of the fin upstream, which can not be discerned in the schlieren photograph. The structure of the flow field obtained by numerical calculation is clearer. It is obvious that the complex wave structure obtained from the leading edge shock wave, the separated shock wave and the intersecting waves can be seen. Compared with the interference flow field of the $\Lambda = 67.5^\circ$ blunt fin, the increase of the sweep angle makes the interference intensity weaken and the interference range decreases obviously. The calculated main separation distance is about 0.8D.

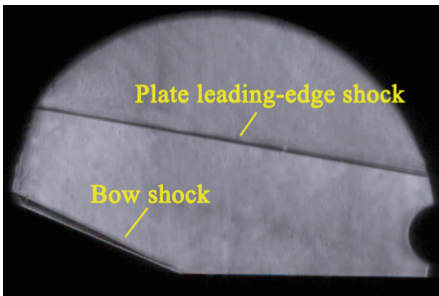


Fig. 16. Schlieren photograph of the $\Lambda = 67.5^\circ$ fin

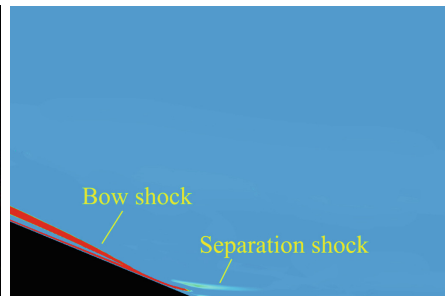


Fig. 17. Density gradient contours of the $\Lambda = 67.5^\circ$ fin

Figures 18 and 19 give the calculated heat flux distributions of the plate central line and the center line of the fin leading edge. It can be seen that the peak value in the center line of the flat and blunt leading edge decreases with the increase of the back sweep angle, and the peak value of the flat center line of the $\Lambda = 67.5^\circ$ blunt fin is only 1/5 of the $\Lambda = 45^\circ$ blunt fin, and the peak of the center line of the fin leading is only about the 1/3 of the $\Lambda = 45^\circ$ blunt fin. The influence range of the interaction flow field on the upstream heat flux rate decreases with the increase of the sweep angle. The $\Lambda = 67.5^\circ$ blunt fin is only about 1/2 of $\Lambda = 67.5^\circ$ blunt fin.

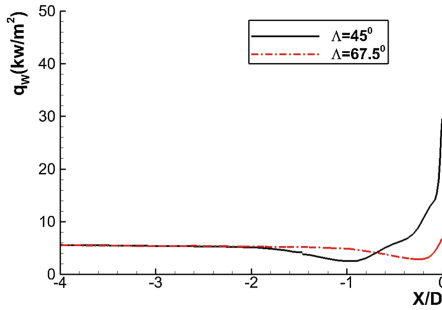


Fig. 18. Heat transfer rate distribution on the centerline of the plate with different sweep angles

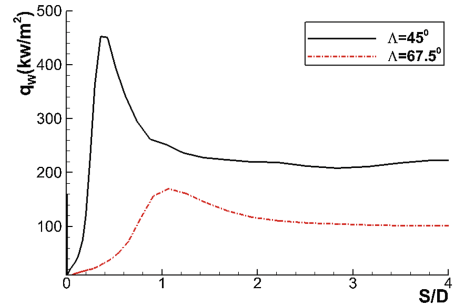


Fig. 19. Heat transfer rate distribution on the centerline of the fin with different sweep angles

4 Conclusions

In this paper, comparing with the typical wind tunnel experimental results, the numerical simulation method is used to study the three-dimensional laminar flow interaction caused by a swept fin mounted on a flat plate. The effects of the grid, numerical scheme and limiter on the calculation results are analyzed. The spatial structure of the interaction flow field of the swept fin and the surface characteristics caused by the shock wave/boundary layer interaction are described. The characteristics of the separation and the influence of sweep angle on the flow field and load distribution are given.

- Mesh density, numerical scheme and combination of limiter all affect the calculation results of the swept fin laminar flow field. Under the same grid density, the combination of the small dissipative numerical scheme with the limiter is closer to the experimental value. But for small dissipative numerical schemes and limiter combinations, with the increase of grid density, computation is prone to oscillations. For such complex flows, numerical scheme, limiter function and other control parameters should be carefully chosen according to actual demand.
- There are complex wave system, vortex structure and separation and reattachment of flow field in the swept fin laminar flow field. Due to the interaction between the fin leading edge shock and the separation shock, the peak value of the pressure and heat transfer rate at the intersection of the fin leading edge and the shock wave occur.
- With the increase of the swept angle of the blunt fin, the interference intensity becomes weaker, and the peak value of separation distance and heat transfer rate decreases obviously.
- For the complex separation flow of this kind of shock wave/boundary layer interaction, it is difficult to find a universal numerical simulation method to ensure the reliability of the results because of the complexity and diversity of the flow structure and the sensitivity to the numerical factors. With the combination of numerical

simulation and experimental measurement, a numerical method which can meet the requirements of a certain precision can be obtained by checking and improving methods and complementary to each other. The interference characteristics such as surface and space structure, load distribution and so on can be more fully understood, and the reference and basis for engineering design are provided.

References

1. Dolling DS (2000) 50 Years of shock wave/boundary layer interaction – what next? AIAA 2000–2569
2. Benek JA (2010) Overview of the 2010 AIAA shock boundary layer interaction prediction workshop. AIAA 2010–4821
3. Brusniak L, Dolling DS (2010) Physics of unsteady blunt-fin-induced shock wave/turbulent boundary layer interactions. *J Fluid Mech*
4. Li SX, Guo XG (2010) Blunt fin induced shock wave/laminar and transitional boundary layer interaction in hypersonic flow. In: Proceedings of the 13th Asian Congress of Fluid Mechanics
5. Li SX (2007) Complex flow dominated by shock wave and boundary layer. Science Press, Beijing (in Chinese)
6. Schuricht PH, Roberts GT (1998) Hypersonic interference heating induced by a blunt fin. AIAA 1998–1579
7. Druguet MC, Candler GV, Nompelis I (2005) Effect of numerics on navier–stokes computations of hypersonic double-cone flows. *AIAA J* 43(3):616–623
8. Yan C (2006) Computational fluid dynamics. Beihang Press, Beijing (in Chinese)
9. Kim KH, Kim C, Rho OH (1998) Accurate computations of hypersonic flows using Ausmpw+ scheme and shock-aligned grid technique. AIAA 1998–2442
10. Ma JK, Li SX (2014) Heat flux measurement in separated flowfield induced by a swept blunt fin. In: 4th international conference on experimental fluid mechanics
11. Li SX, Shi J, Guo XG (2014) Experimental study of the boundary layer features on a flat plate in high speed flow. In: 4th international conference on experimental fluid mechanics